**Supplementary information**

# Experimental

## Sequence alignments

Sequences from different species were aligned using FASTA server,[1] using the following δPKC proteins: human (Q05655), mouse (P28867), rat (P09215), chicken (gi|57524924) and chameleon (G1KHZ5); Myristoylated alanine-rich C-kinase substrate (MARCKS) proteins: human (P29966), mouse (P26645), rat (P30009), chicken (P16527) and chameleon (G1KLW9); Dynamin-1-like protein (Drp1) proteins: human (O00429), mouse (Q8K1M6), rat (O35303), chicken (F1NPT0) and chameleon (G1KMD1); Insulin receptor substrate 1 (IRS1) proteins: human (P35568), mouse (P35569), rat (P35570), chicken (F1NIJ3) and chameleon (G1KC98); Transient receptor potential cation channel subfamily M member 2 (TRPM2) proteins: human (O94759), mouse (O91YD4), rat (Q5G856) and chicken (Q6DMS2); AT-rich interactive domain-containing protein 4A (ARI4A) proteins: human (P29374), mouse (124487105), rat (157820197) and chicken (61098340); Protein lin-28 homolog A (LN28A) proteins: human (Q9H9Z2), mouse (Q8K3Y3), rat (157816953) and chicken (Q45KJ5); Alpha-L-iduronidase (IDUA) proteins: human (P35475), mouse (P48441), rat (285026506) and chicken (71895299); Cdc42-interacting protein 4 (CIP4) proteins: human (Q15642), mouse (Q8CJ53) and rat (P97531); Dynamin-3 (DYN3) proteins: human (Q9UQ16), mouse (Q8BZ98) and rat (Q08877); Dynamin-2 (DYN2) proteins: human (P50570), mouse (P39054), rat (P39052) and chameleon (G1KR95); Myosin light chain (MYLC-2) proteins: human (Q02045), mouse (114326499), rat (386869343) and chicken (148225102); Insulin receptor substrate 2 (IRS2) proteins: human (Q9Y4H2), mouse (P81122) and rat (274323811); Zinc finger protein 638 (ZN638) proteins: human (Q14966), mouse (Q61464) and rat (157823247); Protein kinase C theta (PRKCT) proteins: human (Q04759), mouse (Q02111) and rat (Q9WTQ0); High mobility group protein B3 (HMGB3) proteins: human (O15347), mouse (O54879) and chicken (P40618) and chameleon (H9GJU1); εPKC protein: human (Q02156); βPKC protein: human (P05771) and ξPKC protein: human (68067736).

## Peptide synthesis

In brief: Peptides were synthesized on solid support using a fully automated microwave peptide synthesizer (Liberty, CEM Corporation). The peptides were synthesized by SPPS (solid phase peptide synthesis) methodology[2] with a fluorenylmethoxycarbonyl (Fmoc)/tert-butyl (tBu)

protocol. The final cleavage and side chain deprotection was done manually without microwave energy. Peptides were analyzed by analytical reverse-phase high-pressure liquid chromatography (RP-HPLC) (Shimadzu, MD, USA) and matrix-assisted laser desorption/ionization (MALDI) mass spectrometry (MS) and purified by preparative RP-HPLC (Shimadzu, MD, USA).

Further details: All commercially available solvents and reagents were used without further purification. Dichloromethane (DCM), N-methyl-2-pyrrolidone (NMP), triisopropylsilane (TIS), N,N-diisopropylethylamine (DIEA), O-benzotriazole-N,N,N',N'-tetramethyl-uronium-hexafluoro-phosphate (HBTU), 1-hydroxybenzotriazole (HOBt) and trifluoroacetic acid (TFA) were purchased from Sigma-Aldrich (MO, USA); dimethylformamide (DMF) was purchased from Alfa Aesar (MA, USA); piperidine was purchased from Anaspec (CA, USA); rink amide AM resin was purchased from CBL Biopharma LLC (substitution 0.49 mmol/g, CO, USA); Fmoc-protected amino acids were purchased from Advanced ChemTech and GL Biochem (KY, USA and Shanghai, China). Side chains of the amino acids used in the synthesis were protected as follows: tert-Butyloxycarbonyl (Boc) (Lys/Trp), tert-Butyl (tBu) (Ser/Thr/Tyr), tert-Butyl ester (OtBu) (Asp/Glu), 2,2,4,6,7-pentamethyl-dihydrobenzofuran-5-sulfonyl (Pbf) (Arg) and Trityl (Trt) (Asn/Cys/Gln/His).

Peptides were chemically synthesized using Liberty Microwave Peptide Synthesizer (CEM Corporation, NC, USA) on solid support with an additional module of Discover (CEM Corporation, NC, USA) equipped with fiber-optic temperature probe for controlling the microwave power delivery following the fluorenylmethoxycarbonyl (Fmoc)/tert-butyl (tBu) method in a 30 ml teflon reaction vessel. Each deprotection and coupling reaction was performed with microwave energy and nitrogen bubbling.

Fmoc deprotection was performed in two steps: 30 sec and 180 sec, both at 45 W, 75°C using piperidine (20%) in DMF with HOBt (0.1 M) solution. Coupling reactions were performed by repetition of the following cycle conditions: 300 sec, 25 W, 75°C, with HBTU (0.11 M) in DMF, amino acids (0.12 M) in DMF and DIEA (0.25 M) in NMP solution. The coupling and Fmoc deprotection steps were monitored using Kaiser (ninhydrin) Test[3] and small cleavage. Peptide cleavage from the resin and deprotection of the amino acid side chains were carried out with TFA/TIS/$H_2O$/phenol solution (90:2.5:2.5:5 v/v/v/w) for three hours at room temperature without microwave energy. The crude products were precipitated with diethyl ether, collected by centrifugation, dissolved in $H_2O/CH_3CN$ and lyophilized.

Products were analyzed by analytical reverse-phase high-pressure liquid chromatography (RP-HPLC) (Shimadzu LC-20 equipped with: CBM-20A system controller, SPD-20A detector, CTO-20A column oven, 2 × LC-20AD solvent delivery unit, SIL-20AC autosampler, DGU-20A5 degasser from Shimadzu, MD, USA) using an ultro 120 5 μm C18Q (4.6 mm ID × 150 mm) column (Peeke Scientific, CA, USA) at 1 mL/min. The solvent systems used were A ($H_2O$ with 0.1% TFA) and B ($CH_3CN$ with 0.1% TFA). A linear gradient of 5–50% B in 15 min was applied and the detection was at 215 nm.

The synthesis products were purified by preparative RP-HPLC (Shimadzu LC-20 equipped with: CBM-20A system controller, SPD-20A detector, CTO-20A column oven, 2 × LC-6AD solvent delivery unit and FRC-10A fraction collector from Shimadzu, MD, USA), using an XBridge Prep OBD C18 5 μm (19 mm ID × 150 mm) column (Waters, MA, USA) at 10 mL/min. The solvent systems used were A ($H_2O$ with 0.1% TFA) and B ($CH_3CN$ with 0.1% TFA). For separation, a linear gradient of 5–50% B in 45 min was applied and the detection was at 215 nm.

Peptides were conjugated to $TAT_{47-57}$ (YGRKKRRQRRR) carrier peptide through amide bond, as part of the solid phase peptide synthesis. Note that $TAT_{47-57}$-based delivery of a variety of peptide cargoes into cells has been used now for over 25 years and delivery of the cargo across biological membranes and into subcellular organelles has been confirmed.[4] The peptides were dissolved in water or saline.

## Animal care

Animal care and husbandry procedures were in accordance with the National Institutes of Health guidelines. The animal protocols were approved by the Stanford University Institutional Animal Care and Use Committee.

## Animal studies

All treatments were performed between 9:00 a.m. and 4:00 p.m. by observers blinded to the treatment groups. Male rats were housed in a temperature- and light-controlled room for at least 3 days before use. All animals were randomized and assigned to testing groups to generate biological replicates for each group.

## *Ex vivo* rat heart model of myocardial infarction-induced ischemia and reperfusion injury

Wistar male rats, four to six weeks old, were treated with different peptides or control and the level of phosphorylation, infarct size and creatine kinase (CK) release were measured, as previously described.[5] We excluded hearts if they met one of the following criteria: (1) time to perfusion prior to ischemia and reperfusion protocol exceeded 3 min, (2) coronary flow was outside the range of 9-15 ml/min and (3) heart rate was below 240 beats/min or severe arrhythmia was observed.

An *ex vivo* model of acute ischemic heart injury was carried out as previously described.[6] Briefly, Wistar rats (250-275 g) purchased from Charles River (MA, USA) were heparinized (1000 units/kg; intraperitoneal injection) and then anesthetized with Beuthanasia-D (100 mg/kg intraperitoneal injection). Hearts were rapidly excised and then perfused with an oxygenated Krebs-Henseleit buffer (120 mM NaCl, 5.8 mM KCl, 25 mM $NaHCO_3$, 1.2 mM $NaH_2PO_4$, 1.2 mM $MgSO_4$, 1 mM $CaCl_2$, and 10 mM dextrose, pH 7.4) at 37°C in a Langendorff coronary perfusion system. A constant coronary flow rate of 10 ml/min was used. Hearts were submerged into a heat-jacketed organ bath at 37°C. After 10 min of equilibration, the hearts were subjected to 30 min of global ischemia and 60 min of reperfusion. The hearts were perfused with 500 pM to 1 μM peptides as indicated for 20 min after the ischemia. Normoxic control hearts were subjected to 90 min of perfusion in the absence of ischemia. Coronary effluent was collected to determine CK release during the first 30 min of the reperfusion period. At the end of the reperfusion period, hearts were sliced into 1-mm-thick transverse sections and incubated in triphenyltetrazolium chloride solution (TTC, 1% in phosphate buffer, pH 7.4) at 37°C for 15 min. Infarct size was expressed as a percentage of the risk zone (equivalent to total muscle mass). Infarct size and CK release were used to assess cardiac damage, as described previously.[6] All samples were identical prior to allocation of treatments, and analysis was carried out by an observer blinded to the experimental conditions. ($n \geq 4$ hearts per treatment). Data are presented as mean ± SEM. **$p<0.01$, ***$p<0.005$, ****$p<0.001$ compared to TAT control.

## Western blot analysis

For protein phosphorylation, cardiac fractions were resuspended in buffer A (210 mM mannitol, 70 mM sucrose, 5 mM MOPS, and 1 mM EDTA) in the presence of protease inhibitor and phosphatase inhibitor mixtures (Sigma-Aldrich, MO, USA). Protein content was measured with

the Bradford protein assay. Cell lysates were separated by 10% SDS-PAGE and transferred onto Polyvinylidene difluoride (PVDF) membranes (Millipore, USA). Phosphorylation of δPKC in the *ex vivo* model was determined on 1D SDS PAGE using phospho δPKC (2055, Cell Signaling, MA, USA) and δPKC (C-17, Santa Cruz, CA, USA); phospho IRS1 (2381, Cell Signaling, MA, USA) and IRS1 (SC-559, Santa Cruz, CA, USA); phospho MARCKS (2741, Cell Signaling, MA, USA) and MARCKS (SC-6455, Santa Cruz, CA, USA); phospho Drp1 (3455, Cell Signaling, MA, USA) and Drp1 (611113, BD Transduction, CA, USA); phospho STAT (8826, Cell Signaling, MA, USA) and STAT (SC-346, Santa Cruz, CA, USA) antibodies. The levels of phosphorylated substrates are normalized to total substrate and presented as a ratio to the phosphorylation in hearts subjected to ischemia and reperfusion in the presence of control treatment. The intensity of the spots were measured using NIH ImageJ.[7] Data are representative of at least four independent experiments.

## Western Blot Analysis and 2D Gel Analysis.

For 2D IEF/SDS polyacrylamide gel electrophoresis, the samples were homogenized in buffer consisting of 7 mol/L urea, 2 mol/L thiourea and 4% CHAPS in the presence of protease inhibitor and phosphatase inhibitor mixtures (Sigma-Aldrich, MO, USA). Supernatants were subjected to a first dimensional separation by an IPGphor isoelectric focus power supply using pre-cast Immobilin DryStrip pI 3−10 strips according to the manufacturer's instruction manual (Amersham Biosciences, NJ, USA). 10% SDS gel electrophoresis and Western blotting were carried out using anti-PDK2 (AP9827a, Abgent, CA, USA), anti-phosphothreonine (9381S and 2351S, Cell Signaling, MA, USA), and anti-phosphoserine PKC substrate (2261L, Cell Signaling, MA, USA) antibodies. Phosphatase treatment confirmed that the leftward shift in PDK mobility is due to phosphorylation.[8] The intensity of the spots was measured using NIH ImageJ.[7]

## Interaction of Drp1/δPKC, *in vitro*

To determine the level of Drp1 binding to δPKC in the presence of ψDrp1-Cargo peptide, 200 ng (1.25 μM) recombinant His-Drp1 were incubated with or without the indicated peptides (1 μM) for 120 min at 4°C, prior to adding 200 ng (1.25 μM) recombinant δPKC (Invitrogen, CA, USA) for 120 min at 4°C. Drp1 was immunoprecipitated using His Ni beads (HisPur™ Ni-NTA Superflow Agarose, Thermo Fisher Scientific, MA, USA) and δPKC binding to Drp1 was determined with δPKC (C-17, Santa Cruz, CA, USA) and Drp1 (611113, BD Transduction, CA,

USA) antibodies and then with HRP-conjugated secondary antibody using Western blot analysis. The intensity of the spots were measured using NIH ImageJ.[7] Data are representative of three independent experiments and presented as mean ± SEM. Statistical analysis was performed using two-tailed unpaired Student's t-test.

## Peptides binding to δPKC and εPKC *in vitro*

In brief: Peptides were covalently attached by the amine of the peptide to the carboxyl on the graphene sensor chip. After a rinse in PBS, base-line current levels for the chip were recorded. Next, PBS was aspirated and a 50 µl droplet of the tested protein at the indicated concentrations was applied to the chip and the change in the sensor chip readout was recorded. After data were gathered, the responses of 25 sensors were averaged, and any background drift recorded in PBS was subtracted. A Hill equation fit was used to determine a Kd. Kd values were also calculated by measurement of the Kon and Koff values at a single concentration. This was done by fitting the binding curve to a double exponential function and the first rinse to a single exponential using a single concentration.

Further details: Binding data of δPKC, εPKC and θPKC to immobilized peptides *in vitro* was gathered using an AGILE Dev Kit label-free binding assay (Nanomedical Diagnostics Inc, CA, USA). The AGILE assay is based on a three terminal liquid gated graphene field effect transistor. This technology has been used for several years and is exquisitely sensitive to fluctuations in the charge profile at the graphene-liquid interface, which lends this modality a high aptitude for sensing charged biomolecules and their dynamics.[9] The current through the sensors and the capacitance between the sensor and the applied liquid is measured continuously. A built in potentiostat controls the potential differences between the liquid and the sensors. Changes in these values are due to binding or other chemical changes on the surface of the chip. Functionalization of the sensor chip with specific capture molecules imparts the sensitivity and selectivity of that capture molecule to the sensor.

Several chemistry steps are employed to functionalize the graphene devices for use as biosensors. Sensor chips come prepared with carboxylic acid anchor sites for biomolecule binding on the graphene transistors. Following the standard protocol from the sensor chip manufacturer, the capture molecules are bound to the chip with a zero length linker (EDC/sulfo-NHS). Provided blocking and quench solutions are used prior to sensor calibration and measurement.

The biosensing measurement is comprised of a voltage sweep by the potentiostat while measuring the current through the sensors. The voltage difference between the liquid and the sensor creates a gate response in the transistor, altering the resistance of the sensor. A layer of capture biomolecules at the interface between bulk liquid and the transistor introduces a competing gating effect, further changing the resistance of the sensor.

The value of the sensor response (I-response) is normalized to zero at calibration. After calibration, the sensor response is the percent change in the current through the transistor. This may be a positive or negative change depending on the exact charges near the transistor. The total magnitude of the response is also dependent on the exact configuration of charges near the transistor. The sensor response for a given capture molecule will be repeatable from chip to chip as long as the same functionalization protocol is followed for each chip.

The introduction of a target species that binds to the layer of capture molecules induces a conformational change in the layer of biomolecules, again shifting the gating profile presented to the transistor. At this step, the change in the transistor resistance is proportional to the number of target molecules bound to capture molecules on the surface. By recording the transistor resistance in real time, the change in binding over time can be recorded and the binding and disassociation rates can be extracted. The specific value of the sensor response varies with the target molecule, but will be repeatable provided the same capture molecule and functionalization chemistry is used. By recording a baseline level before and after introduction of the target species, repeatable and concentration dependent changes in sensor resistance and capacitance are correlated with the overall kinetic chemical binding properties of the capture and target molecules. The association and dissociation rates are calculated using least squares fitting of the sensor data to first order kinetics. In this way ka, kd and kD can be calculated.

1-Ethyl-3-(3-dimethylaminopropyl)carbodiimide (EDAC) (2 mg) and sulfo-N-Hydroxysuccinimide (sNHS) (6 mg) from Sigma-Aldrich (MO, USA) were used in MES buffer (pH 6.0, 5 ml) for 15 min to covalently attach the amine of the peptide the carboxyl on the chip. Peptide solution (6 μM) was incubated with the chip for 15 min. Next, an amine terminated short chain poly-ethylene glycol (3 mM) followed by ethylamine (1 M) were applied serially for 15 min each to quench remaining unoccupied binding sites on the chip. After a rinse in PBS, base-line current levels for the chip were recorded for at least 7 min. Next, the PBS was aspirated and a 50 μl droplet of the tested protein (75 μg/mL, recombinant δPKC, Invitrogen, CA, USA) was applied

to the chip and the change in the sensor chip readout was recorded for 15 min after that the protein was aspirated and the chip was rinsed with PBS. Additional measurements were performed using varying concentrations or using recombinant δPKC (75 μg/mL, recombinant δPKC, Invitrogen, CA, USA) and a peptide (10 μM), or using recombinant εPKC (75 μg/mL, GenWay, CA, USA) and θPKC (75 μg/mL, life technologies, CA, USA) as controls. After data were gathered, the responses of 25 sensors on a single assay chip were averaged, and any background drift recorded in PBS was subtracted. A Hill equation fit was used to determine a Kd. Kd values were also calculated by measurement of the Kon and Koff values at a single concentration. This was done by fitting the binding curve to a double exponential function and the first rinse to a single exponential using a single concentration, and values obtained by these calculation methods were almost identical. Data presented as mean ± SEM of ~25 measurements. All samples were identical prior to allocation of treatments, and analysis was carried out by an observer blinded to the experimental conditions.

## Cell Culture and Ischemia Reperfusion Damage

H9c2 cells were grown in standard DMEM culture media containing 10% fetal bovine serum (FBS) and 1% penicillin-streptomycin. Cells were plated in a black, clear bottom 96-well plates at a density of 7,500 cells per well and incubated overnight in a 37°C incubator. Cells undergoing hypoxia were incubated in serum-free media (DMEM with 1% penicillin-streptomycin) and placed in a GasPak EZ Anaerobe pouch (BD and Company, Franklin Lakes, NJ) for 24 hours at 37°C. Cells undergoing normoxia were incubated in standard culture media for 24 hours at 37°C. For reoxygenation, cells were removed from the GasPak EZ Anaerobe pouch and incubated in standard culture media at 37°C for 2 hours either in the presence or absence of peptides.

## Measurement of mitochondrial reactive oxygen species production

H9c2 cells from above were incubated with 500 ng/mL Hoechst 33342 (Thermosphere, Waltham, MA) and 2.5 μM Mitosis Red (Thermosphere, Waltham, MA) in standard culture media for 30 minutes at 37°C. Cells were then washed three times with Hank's balanced salt solution (HBSS). Overall Mitosis Red and Hoechst 33342 fluorescence was measured using a Spectra ax fluorescence microplate reader (Molecular Devices, Sunnyvale, CA).

## Measurement of spectra max fluorescence microplate reader

H9c2 cells from above were incubated with WST-8 dye (Cell Counting Kit-8, Domino, Kumamoto, Japan) according to manufacturer's instructions. WST-8 reduction was measured at 450 nm absorption using a Spectra ax fluorescence microplate reader (Molecular Devices, Sunnyvale, CA).

## Measurement of cell viability

H9c2 cells from above were incubated in 4% paraformaldehyde in standard culture media at 37°C for 10 minutes and washed three times with phosphate-buffered saline (PBS). Cells were then stained with 500 ng/mL Hoechst 33342 (Thermosphere, Waltham, MA) and 1.5 μM propidium iodide (Thermosphere, Waltham, MA) for 5 minutes. Cells were washed for three more times with PBS and imaged using a Keyence BZ-X700 microscope. Relative propidium iodide intensity was measured using a MATLAB script.

## Statistical analysis

Data are provided as means ± SEM; the number of independent experiments performed is provided in each data set. Data were tested for significance by using the two-tailed unpaired Student t-test. Differences were considered statistically significant when p values were $<0.05$. Sample sizes were estimated based on previous experience with similar assays and the effect of size observed in preliminary experiments.

# Supplementary Tables and Figures

## Table S1. MS and HPLC characterization of the peptides in this study

| Peptide | Sequence | MS. Cal. | MS Obs. | HPLC |
|---|---|---|---|---|
| TAT | YGRKKRRQRRR | 1558.8740 | 1558.1267 | 95% |
| ψMARCKS-Cargo | KAAEEP | 684.7480 | 685.1657 | 98% |
| ψDrp1-Cargo | YTDFDE | 829.8170 | 829.9458 | 98% |
| YTAFDE | YTAFDE | 785.8080 | 785.9678 | 99% |
| YTDFAA | YTDFAA | 727.7720 | 727.6001 | 99% |
| ψIRS1-Cargo | FRPRSKS | 918.0710 | 918.8325 | 98% |
| ψMARCKS | KAAEEP-GG-YGRKKRRQRRR | 2340.6950 | 2341.1673 | 92% |
| ψDrp1 | YTDFDE-GG-YGRKKRRQRRR | 2485.7640 | 2486.2958 | 93% |
| YTAFDE-TAT | YTAFDE-GG-YGRKKRRQRRR | 2528.8330 | 2529.1378 | 99% |
| YTDFAA-TAT | YTDFAA-GG-YGRKKRRQRRR | 2470.7970 | 2471.2370 | 99% |
| ψIRS1 | FRPRSKS-GG-YGRKKRRQRRR | 2574.0180 | 2574.6592 | 93% |

MS was done using MALDI technique and purity was determined by analytical HPLC (for chemical structure see Figure 3).

**Table S2. kD value of δPKC binding to ψMARCKS-Cargo, ψDrp1-Cargo, and ψIRS1-Cargo peptides**

| δPKC - kD (nM) | | | | | | | | |
|---|---|---|---|---|---|---|---|---|
| **Peptide** | **Study 1** | | **Study 2** | | **Study 3** | | **Average** | |
| | **Result** | SD | **Result** | SD | **Result** | SD | **Result** | SD |
| ψMARCKS-Cargo | 8.870 | 2.390 | 11.714 | 3.410 | 3.926 | 1.250 | **8.2** | 2.4 |
| ψDrp1-Cargo | 2.060 | 0.930 | 1.169 | 0.188 | 1.217 | 0.030 | **1.5** | 0.4 |
| ψIRS1-Cargo | 9.180 | 2.750 | 16.200 | 5.340 | 5.229 | 0.924 | **10.2** | 3.0 |

Three independent studies measuring kD of δPKC using varying concentrations to ψMARCKS-Cargo, ψDrp1-Cargo, and ψIRS1-Cargo peptides.

## Figure S1. Rational design of an inhibitors of Drp1 phosphorylation by δPKC

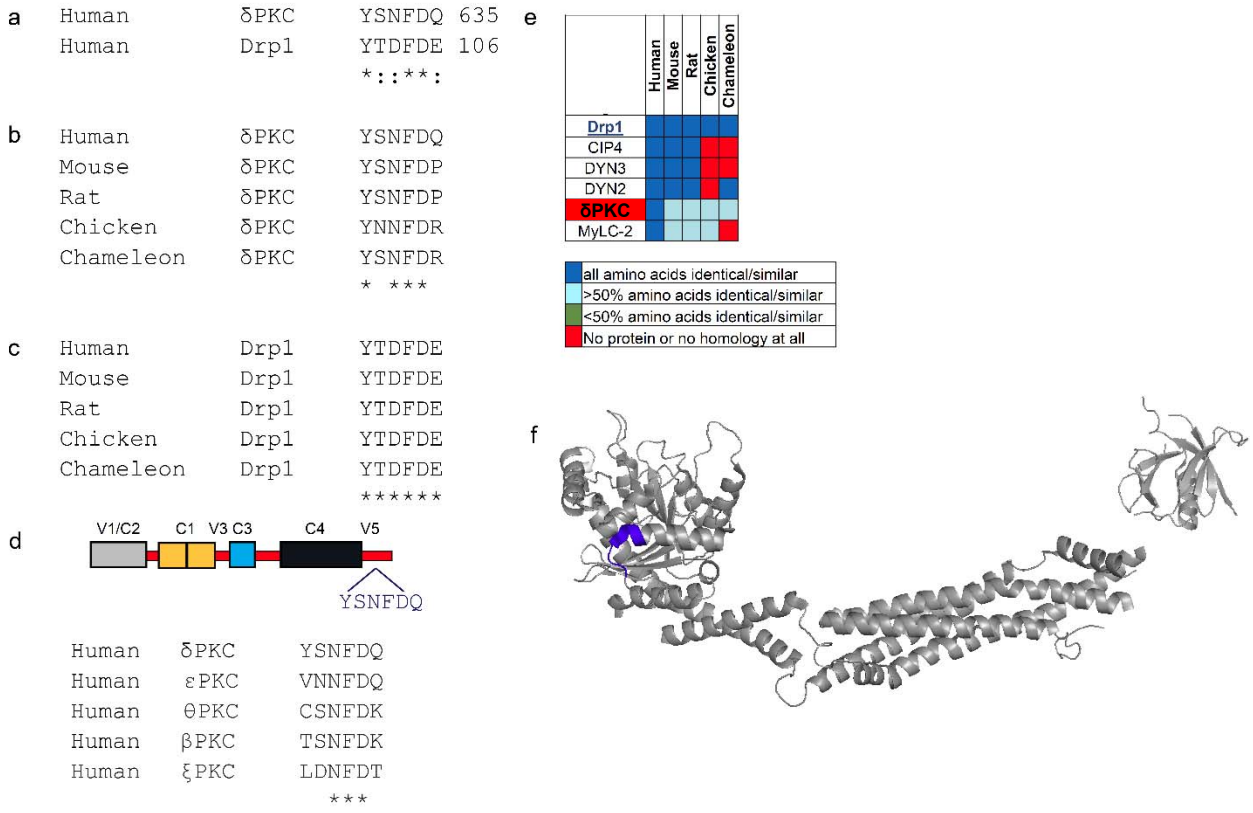


(a) Sequence alignment of human δPKC and Drp1 identified a short sequence of homology, YSNFDQ/YTDFDE. (b) Conservation of YSNFDQ sequence in δPKC and (c) conservation of YTDFDE in Drp1 in a variety of species. (d) YSNFDQ sequence is found in the V5 domain of δPKC. YSNFDQ sequence is not present in other PKC isozymes, including θPKC, the most homologous PKC isozyme to δPKC,[10] εPKC, which is also a member of the novel PKC isozymes, βPKC, member of the conventional PKC class, and ξPKC member of the atypical PKCs. (e) YSNFDQ and YTDFDE sequences are found in 6 human proteins (Drp1, δPKC and 4 other proteins). A heat map of the YSNFDQ and YTDFDE conservation in orthologs of these proteins shows that YSNFDQ and YTDFDE are conserved only in δPKC and Drp1. (f) YTDFDE (blue) in Drp1 (PDB: 3ZVR) is exposed and available for protein-protein interactions. *denotes identity and :denotes homology.

## Figure S2. Rational design of an inhibitors of IRS1 phosphorylation by δPKC

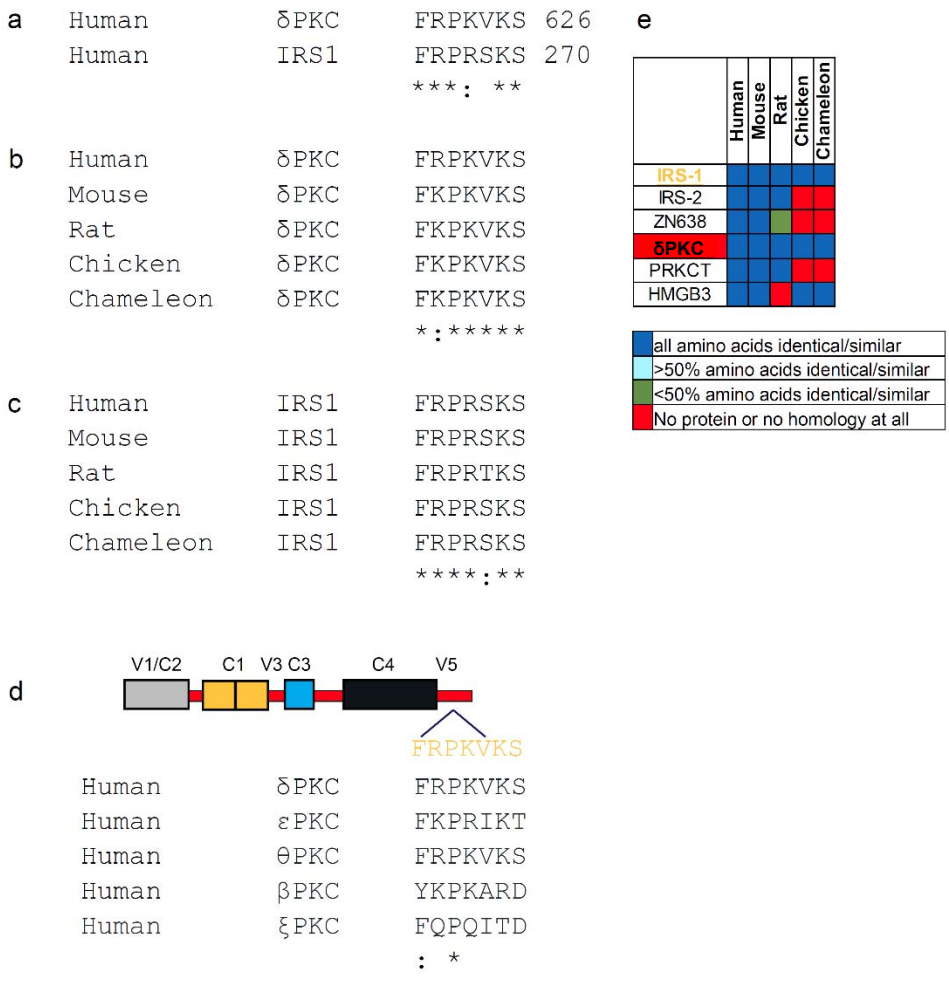


(a) Sequence alignment of human δPKC and IRS1 identified a short sequence of homology, FRPKVKS/ FRPRSKS. (b) Conservation of FRPKVKS sequence in δPKC and (c) conservation of FRPRSKS in IRS1 in a variety of species. (d) FRPKVKS sequence is found in the V5 domain of δPKC. FRPKVKS sequence is less conserved in most other PKC isozymes. (e) FRPKVKS and FRPRSKS sequences are found in 6 human proteins (IRS1, δPKC and 4 other proteins). A heat map of the FRPKVKS and FRPRSKS conservation in orthologs of these proteins shows that FRPKVKS and FRPRSKS are conserved only in δPKC and IRS1. *denotes identity and :denotes homology.

**Figure S3. Dissociation curve of the peptides *in vitro***

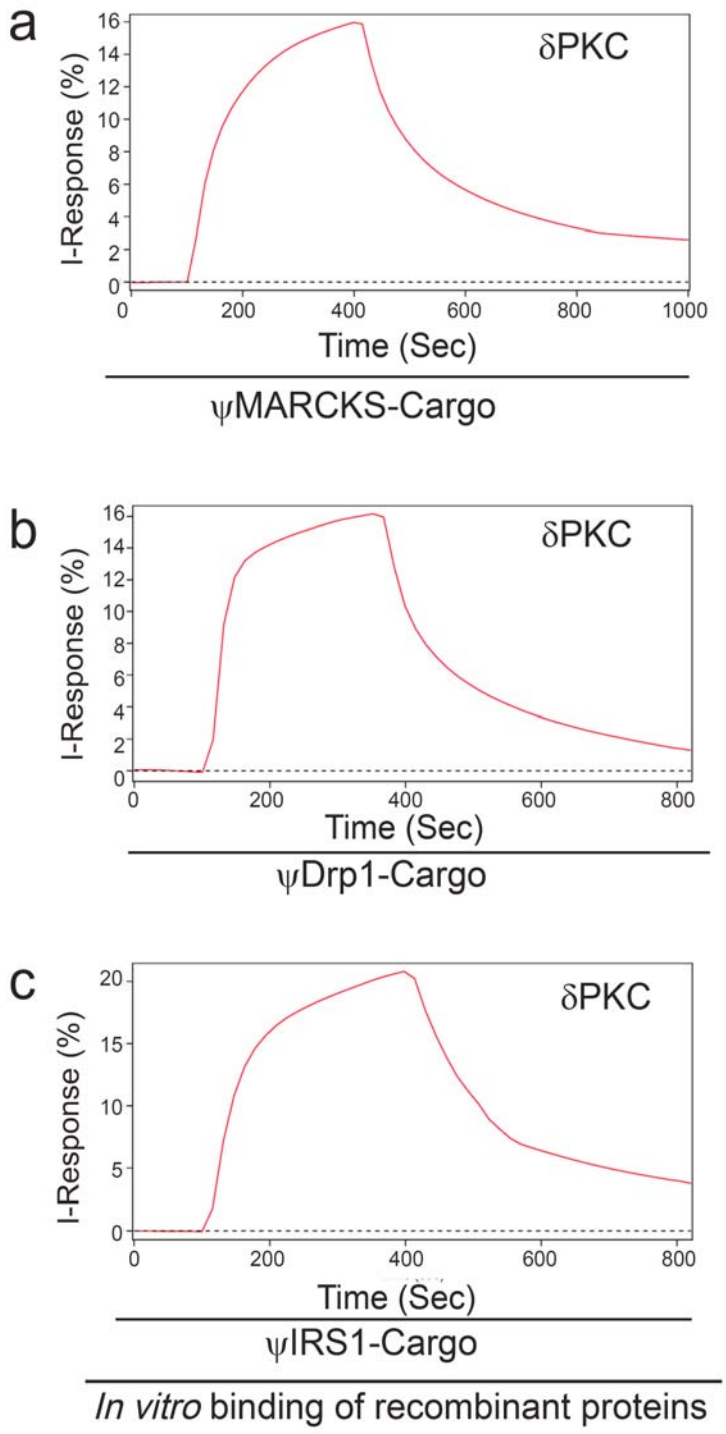


Combined association and dissociation curves of δPKC at ~ 75 µg/mL (~1 µM), to ψMARCKS-Cargo (a), ψDrp1-Cargo (b), and ψIRS1-Cargo (c) peptides.

**Figure S4. ψDrp1-Cargo peptide inhibits the interaction between δPKC and Drp1 *in vitro***

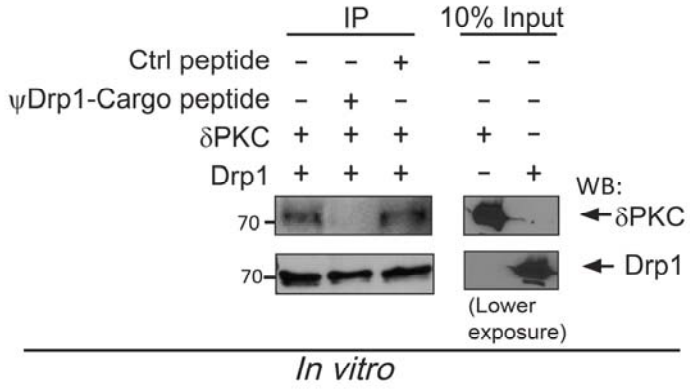


ψDrp1-Cargo peptide (1 μM) inhibited Drp1 and δPKC interaction *in vitro*, determined by co-immunoprecipitation (IP) and Western blotting (WB) analysis (Ctrl peptide=control peptide, YTDFAA; ψIRS1-Cargo peptide) (n=3).

**Figure S5. ψDrp1 and ψIRS1 peptides reduce mitochondrial function following ischemia and reoxygenation, a culture model of cardiac ischemia and reperfusion injury**

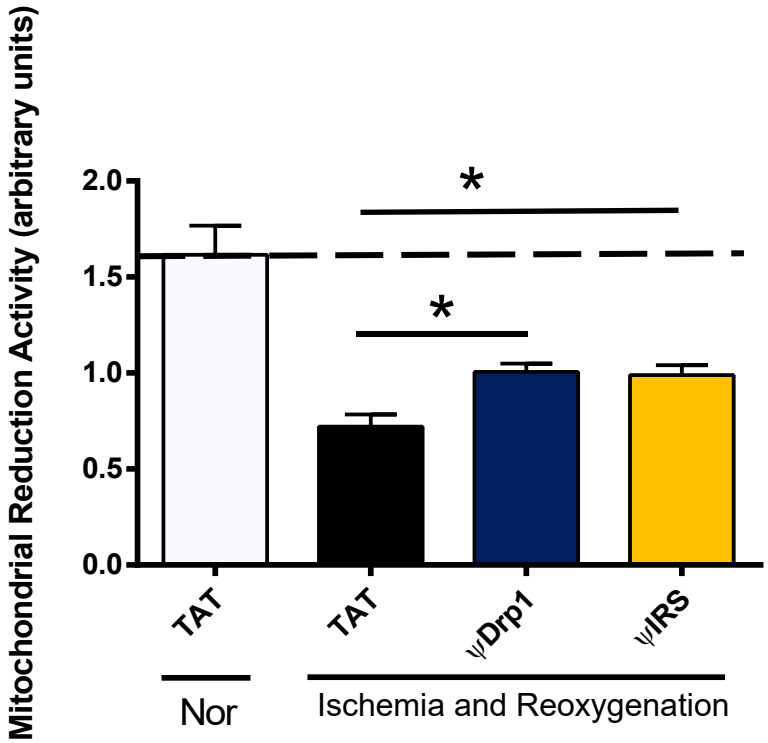


H9c2 cardiac cells were subjected to 26 hours of culturing under normoxic conditions (Nor) or 24 hours of hyopxia and 2 hours of reoxygenation. 1 μM of each peptide were added during the ischemia and reoxygenation insult. Mitochondrial dehydrogenase activity, a surrogate maker for mitochondrial metabolic activity and cell viability, was measured using WST-8, a tetrazolium salt that is reduced in the presence of NADH and NADPH, therefore indicating redox potential and mitochondrial health.[11] Ischemia and reoxygenation damage decreased WST-8 staining, and treatment either ψDrp1 or ψIRS1 peptides decreased mitochondrial dysfunction. Treatment with ψDrp1 or with ψIRS1 reduced ischemia and reoxygenation induced mitochondrial dysfunction. Data are average of percent cell death; are n = 3 per condition. *$p<0.05$ compared to TAT control.

**Figure S6. ψDrp1 and ψIRS1 peptides rescue cell viability following ischemia and reoxygenation, a culture model of cardiac ischemia and reperfusion injury**

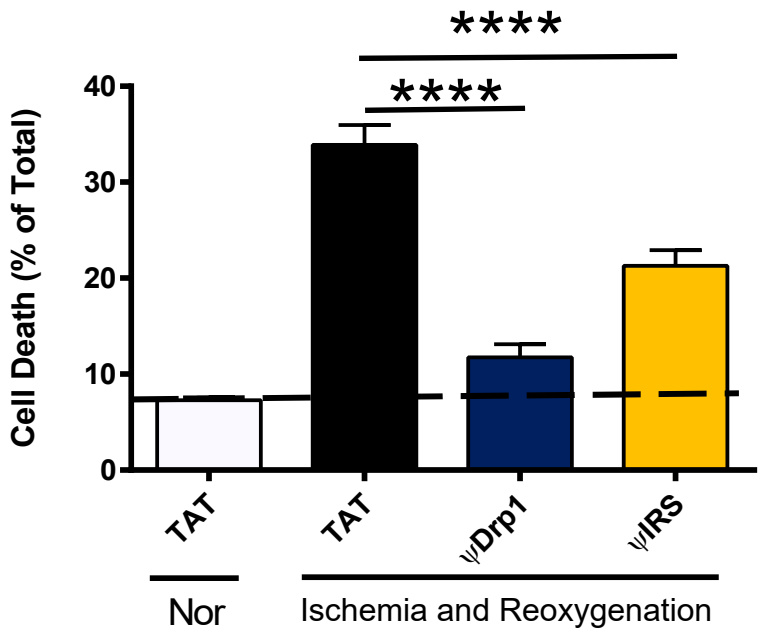


H9c2 cardiac cells were subjected to 26 hours of culturing under normoxic conditions (Nor) or 24 hours of hyopxia and 2 hours of reoxygenation. 2 μM of each peptide were added only during the reoxygenation period. Cell viability was measured as a ratio of Hoechst 33342 staining, a cell permeating dye that stains nuclei of both live and dead cells, and propidium iodide, a cell impermeating dye that stains nuclei of only dead cells. A summary of the fraction of dead cells in each condition. Treatment with ψDrp1 and reduced ischemia and reoxygenation induced cell death by ~80% and ψIRS1 – by ~40%. Data are average of percent cell death; n = 3 per condition, approximately 4,000 cells were counted per condition in each experiment. ****$p<0.001$ compared to TAT control.

**Figure S7. ψDrp1-Cargo and ψIRS1-Cargo peptides (without TAT) are not cardio-protective in the *ex vivo* rat heart ischemia and reperfusion model**

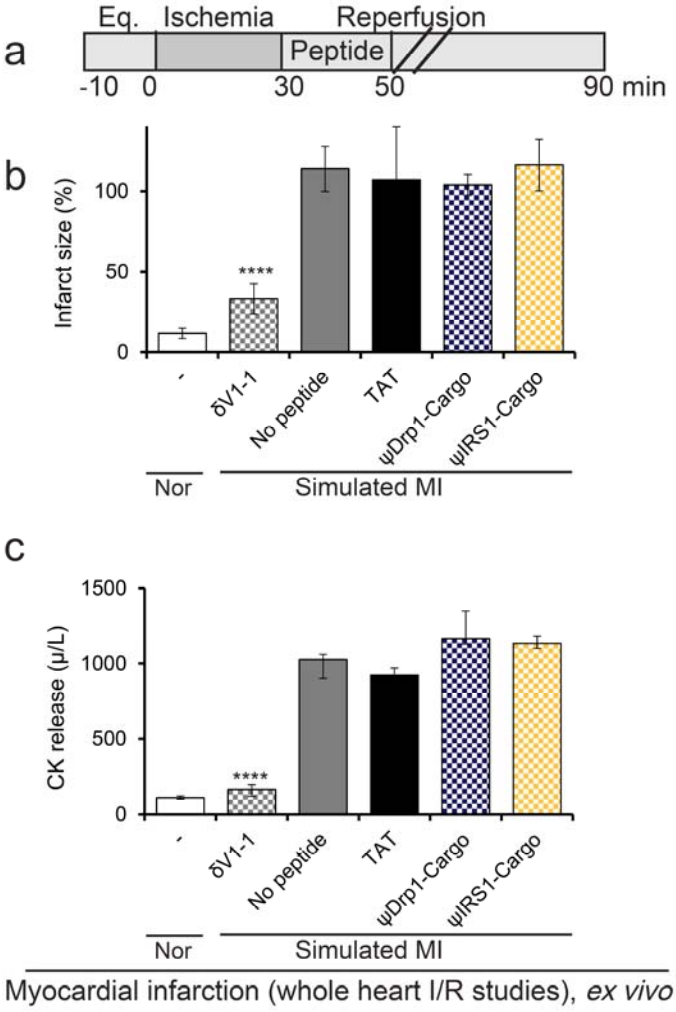


(a) Protocol of myocardial infarction model using isolated hearts subjected to ischemia and reperfusion (a model of simulated myocardial infarction; Simulated MI) or normoxia (Nor). Horizontal bars indicate the length (in minutes) of each treatment (eq = equilibration). Rat hearts were subjected to 30 minutes ischemia followed by 60 minutes reperfusion without or with peptide treatment for the first 20 min only. Protection from myocardial injury was determined by analyses of the levels of (b) infarct size and (c) release of CK with or without corresponding peptides (1 μM). ψDrp1-Cargo and ψIRS1-Cargo peptides lacking the cell-permeable TAT did not have any cardio-protective effect in the *ex vivo* assay. δV1-1 (1 μM), a general inhibitor of δPKC, decreased infarct size by ~70%, as compared to treatment with hearts treated with TAT peptide; measurement in whole heart subjected to simulated myocardial infarction *ex vivo*. Data are presented as mean ± SEM (n = 4 hearts per treatment) ****$p<0.001$ compared to TAT control.

**Figure S8. Selectivity of peptides as phosphorylation inhibitors; phosphorylation of PDK, δPKC substrate, following simulated myocardial infarction**

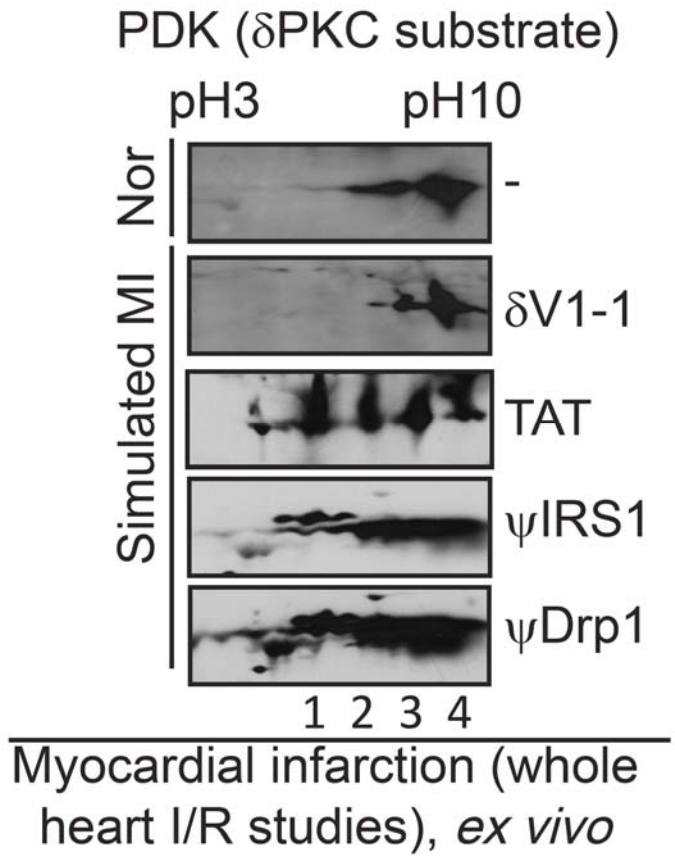


Phosphorylation of PDK after cardiac ischemia and reperfusion in the presence of control or the indicated peptides (1 μM). ψIRS1 and ψDrp1 did not affect the phosphorylation of PDK. The two-dimensional polyacrylamide gel electrophoresis (PAGE) allows the separation of PDK phosphorylation states from the lowest, spot 4, to the highest, spot 1.

**Figure S9. Phosphorylation of Drp1 following simulated myocardial infarction**

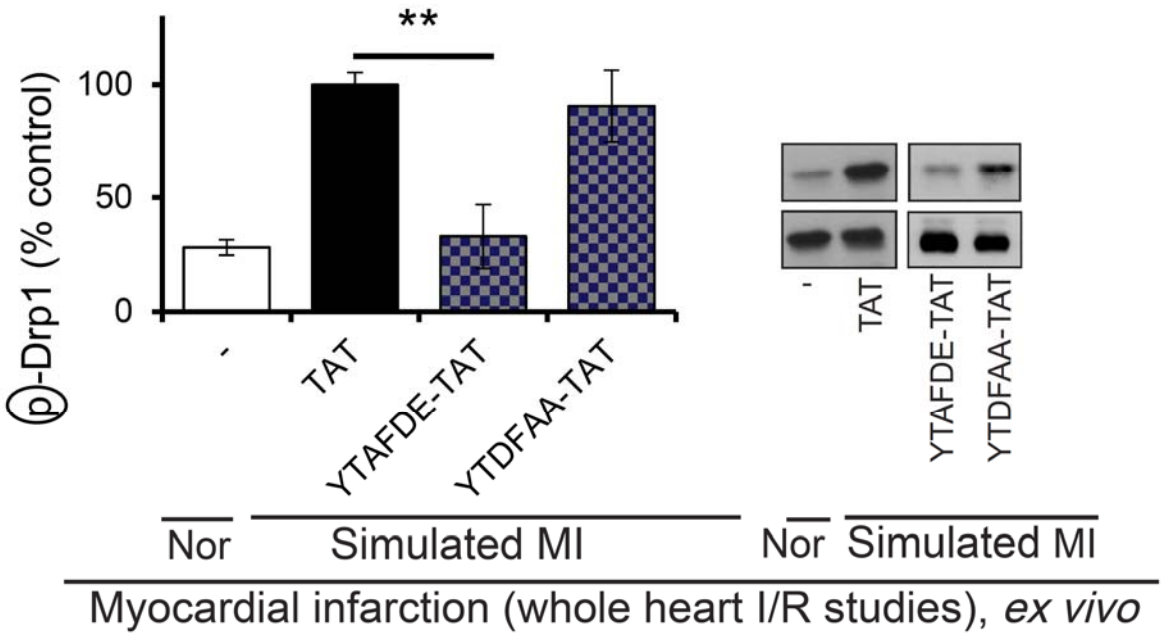


Phosphorylation of Drp1 after cardiac ischemia and reperfusion in the presence of control (TAT) or two ψDrp1 analogs (YTAFDE-TAT or TYTDFAA-TAT, each at 1 μM). Phosphorylation is expressed as a percent change from control (TAT)-treated hearts subjected to ischemia and reperfusion, as in Figure 7.

**Figure S10. A dose response study for ψDrp1, ψIRS1 and for the combination of the peptides (ψDrp1 together with ψIRS1) peptides in the *ex vivo* rat heart ischemia and reperfusion model**

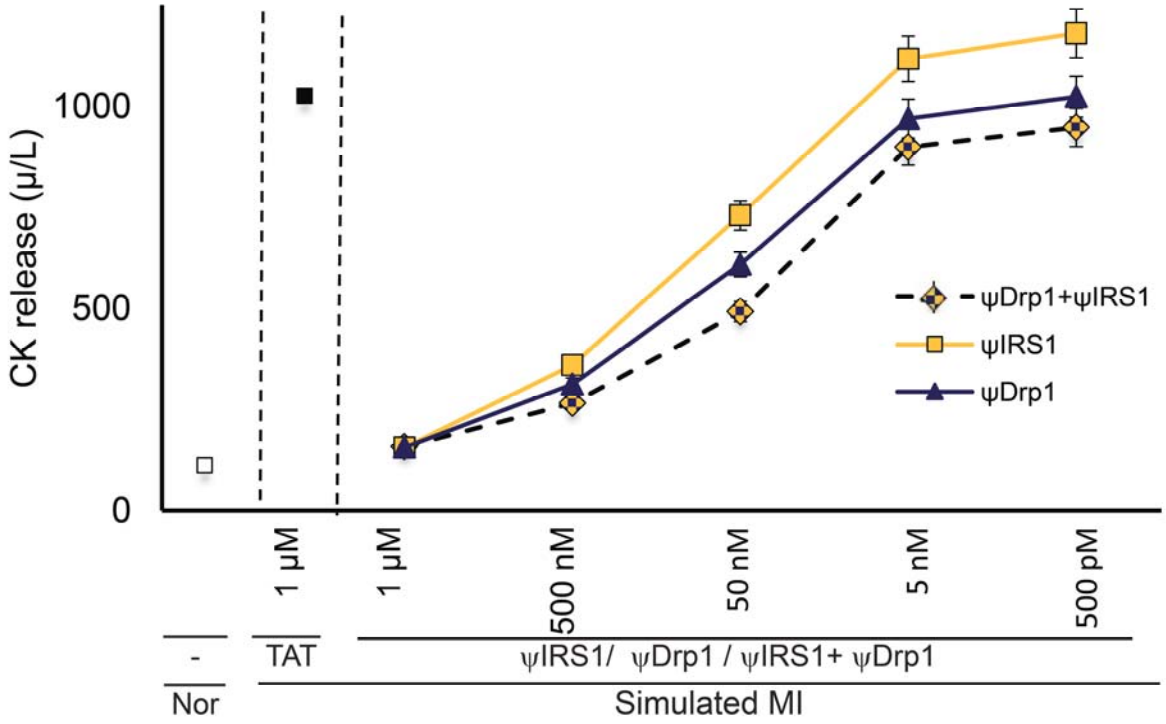


A dose-response study demonstrated that ψDrp1 (blue triangle) and ψIRS1 (orange rectangle) are highly active; the $IC_{50}$ for ψDrp1 peptide effect in reducing cardiac injury *ex vivo* was ~100 nM and the $IC_{50}$ for ψIRS1 was ~350 nM, as demonstrated by cardiac CK release, a clinical biomarker for heart attack. Interestingly, a combination of ψDrp1 and ψIRS1 (blue and orange diamond) appears to be superior effect as compared with each peptide alone, with an $IC_{50}$ of ~50 nM.

# References


[1] W. R. Pearson, D. J. Lipman, *Proc. Natl. Acad. Sci. U. S. A.* **1988**, *85*, 2444-2448.

[2] R. B. Merrifield, *J. Am. Chem. Soc.* **1963**, *85*, 2149-2154.

[3] E. Kaiser, R. L. Colescot, C. D. Bossinge, P. I. Cook, *Anal. Biochem.* **1970**, *34*, 595-598.

[4] aR. Begley, T. Liron, J. Baryza, D. Mochly-Rosen, *Biochem. Biophys. Res. Commun.* **2004**, *318*, 949-954; bM. Rizzuti, M. Nizzardo, C. Zanetta, A. Ramirez, S. Corti, *Drug discovery today* **2015**, *20*, 76-85; cP. Lonn, S. F. Dowdy, *Expert opinion on drug delivery* **2015**, *12*, 1627-1636.

[5] aK. Inagaki, H. S. Hahn, G. W. Dorn, 2nd, D. Mochly-Rosen, *Circulation* **2003**, *108*, 869-875; bK. Inagaki, L. Chen, F. Ikeno, F. H. Lee, K. Imahashi, D. M. Bouley, M. Rezaee, P. G. Yock, E. Murphy, D. Mochly-Rosen, *Circulation* **2003**, *108*, 2304-2307.

[6] L. Chen, L. R. Wright, C. H. Chen, S. F. Oliver, P. A. Wender, D. Mochly-Rosen, *Chem. Biol.* **2001**, *8*, 1123-1129.

[7] M. D. Abràmoff, P. J. Magalhães, S. J. Ram, *Biophotonics international* **2004**, *11*, 36-43.

[8] E. N. Churchill, C. L. Murriel, C. H. Chen, D. Mochly-Rosen, L. I. Szweda, *Circ. Res.* **2005**, *97*, 78-85.

[9] aC. Mackin, T. Palacios, *Analyst* **2016**, *141*, 2704-2711; bM. B. Lerner, F. Matsunaga, G. H. Han, S. J. Hong, J. Xi, A. Crook, J. M. Perez-Aguilar, Y. W. Park, J. G. Saven, R. Liu, A. T. Johnson, *Nano letters* **2014**, *14*, 2709-2714; cY. Huang, X. Dong, Y. Liu, L.-J. Li, P. Chen, *Journal of Materials Chemistry* **2011**, *21*, 12358-12362.

[10] L. Chen, H. Hahn, G. Wu, C. H. Chen, T. Liron, D. Schechtman, G. Cavallaro, L. Banci, Y. Guo, R. Bolli, G. W. Dorn, 2nd, D. Mochly-Rosen, *Proc. Natl. Acad. Sci. U. S. A.* **2001**, *98*, 11114-11119.

[11] M. V. Berridge, A. S. Tan, K. D. McCoy, M. Kansara, F. Rudert, *J. Immunol.* **1996**, *156*, 4092-4099.